

# *Development and Application of an ALE Large Deformation Formulation*

Y. Tadi beni<sup>i</sup>; M. R. Movahhedy<sup>ii</sup>; and G.H. Farrahi<sup>iii</sup>

## **ABSTRACT**

This paper presents a complete derivation and implementation of the Arbitrary Lagrangian Eulerian (ALE) formulation for the simulation of nonlinear static and dynamic problems in solid mechanics. While most of the previous work done on ALE for dynamic applications was mainly based on operator split and explicit calculations, this work derives the quasi-static and dynamic ALE equations in its simple and correct form, using a fully coupled implicit approach. Full expression for the ALE virtual work equations is given. Time integration relations for the dynamic equations are also derived. Examples of quasi-static and dynamic large deformation applications are presented.

## **KEYWORDS**

FEM, ALE, Large deformation, Coupled formulations, implicit dynamic analysis.

## **1. INTRODUCTION**

The Arbitrary Lagrangian Eulerian (ALE) formulation has emerged in recent years as a technique that can alleviate many of the drawbacks of the traditional Lagrangian and Eulerian formulations [1-6,11]. In the ALE analysis, the finite element mesh is neither attached to the material nor fixed in space, but each degree of freedom of the system may be assigned an arbitrary motion independent of the material deformation. Therefore, ALE is a general formulation that can be reduced to Eulerian or Lagrangian formulation as special cases. By combining the merits of both the Lagrangian and Eulerian formulations, ALE can easily describe different types of boundary conditions and prevent mesh distortion. The ALE equations are derived by substituting the relationship between the material time derivative and grid time derivative into the governing equations of continuum mechanics. The various ALE procedures in the literature may be divided into two categories. In one category, an operator-split approach is used in which each step of the analysis is decoupled into a Lagrangian step and a convection step. In the former step, the solution to

Lagrangian motion is obtained, and in the latter step the solution is mapped to the desired mesh to complete the ALE step [4, 2]. In the second category, a fully coupled approach is used that represents a true kinematic description where material deformation is described relative to a moving reference configuration. While the first approach is computationally convenient, it reduces the accuracy of the analysis [2]. In fact, the operator-split approach may not be called a strictly ALE approach, since it is practically equivalent to an updated Lagrangian formulation followed by consecutive remeshing. In contrast, the fully coupled approach is a true ALE formulation, because in this approach the grid and material motion occur simultaneously.

Many of the ALE formulations presented in the literature consider only quasi-static deformation. In recent years a few dynamic formulations have appeared [1]. In this work, a complete formulation of the fully coupled implicit dynamic ALE formulation is presented. Virtual work equations are first derived from the basic principles of continuum mechanics and are presented in simplified form compared to the previous works. Examples of quasi-static and dynamic large deformation applications are solved and discussed.

---

<sup>i</sup> Y. Tadi beni is Ph.D. Student in the Department of Mechanical Engineering, Sharif University of Technology, Tehran, Iran (e-mail: yaghob\_beni@mech.sharif.edu)

<sup>ii</sup> M. R. Movahhedy is Associate professor in the Department of Mechanical Engineering, Sharif University of Technology, Tehran, Iran (e-mail: movahhed@sharif.edu)

<sup>iii</sup> G.H. Farrahi is Professor in the Department of Mechanical Engineering, Sharif University of Technology, Tehran, Iran (e-mail: farrahi@sharif.edu)

## 2. DESCRIPTION OF MOTION IN THE ALE

### Kinematics

In the ALE description of motion, neither the material configuration  $X$  nor the spatial configuration  $x$  is taken as the reference. Instead, a third domain, called the referential configuration  $\chi$  is used. In this description, the material configuration is identified by a set of material point coordinates  ${}^t x_i^m$  while the reference configuration, or grid, is identified by an independent set of grid point coordinates  ${}^t x_i^g$ . Figure 1 shows the one-to-one mapping that relates the three configurations.

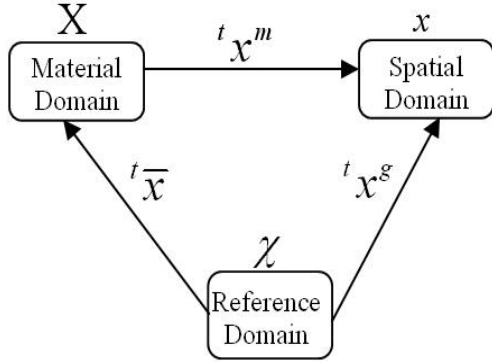


Figure 1: Schematic diagram of the mapping between the three domains in the ALE description

The referential domain  $\chi$  is mapped into the material and spatial domains by  $\bar{x}$  and  ${}^t x^g$ , respectively. The domain of the material points,  $X$ , is related to the spatial points,  $x$ , by

$${}^t x_i = {}^t x_i^m(X_j, t) \quad (1)$$

The mapping of  ${}^t x^g$  from the referential domain to the spatial domain, which can be understood as the motion of the grid points in the spatial domain, is represented by

$${}^t x_i = {}^t x_i^g(\chi_j, t) \quad (2)$$

The material velocity  ${}^t v_i$ , the grid point velocity  ${}^t v_i^g$ , and the convective velocity  ${}^t c_i$  at time  $t$  are given by

$${}^t v_i = \frac{\partial {}^t x_i^m}{\partial t} \Big|_{X_j}, \quad {}^t v_i^g = \frac{\partial {}^t x_i^g}{\partial t} \Big|_{\chi_j}, \quad {}^t v_i - {}^t v_i^g = {}^t c_i \quad (3)$$

In addition, the boundaries of the material and grid configurations should coincide, i.e.

$$({}^t v_i - {}^t v_i^g) {}^t n_i \Big|_{on-the-boundary} = 0 \quad (4)$$

where  ${}^t n_i$  is the unit normal vector at any point on the boundary. The material time derivative and grid time derivative of an arbitrary function  ${}^t f$  are given by

$${}^t \dot{f} = \frac{\partial {}^t f}{\partial t} \Big|_{X_i}, \quad {}^t f' = \frac{\partial {}^t f}{\partial t} \Big|_{\chi_i} \quad (5)$$

The fundamental ALE relation between material time derivatives and grid time derivatives is given by reference [7]

$${}^t \dot{f} = {}^t f' + ({}^t v_i - {}^t v_i^g) \frac{\partial {}^t f}{\partial {}^t x_i} \quad (6)$$

The local form of conservation of mass, continuity, at time  $t$  is given by

$${}^t \dot{\rho} = -{}^t \rho \frac{\partial {}^t v_i}{\partial {}^t x_i} \quad (7)$$

where  ${}^t \rho$  is the material density. Using (6), the ALE form of the continuity equation can be expressed as

$${}^t \rho' = -{}^t \rho \frac{\partial {}^t v_i}{\partial {}^t x_i} - {}^t c_i \frac{\partial {}^t \rho}{\partial {}^t x_i} \quad (8)$$

## 3. DERIVATION OF ALE EQUATION OF MOTION

### Virtual work

In the dynamic analysis, inertia effects are included in the equation of balance of momentum. The governing equations are expressed at time  $t + \Delta t$ , but the configuration at time  $t + \Delta t$  is yet unknown. Referring all variables to the grid configurations at time  $t$  and linearizing the equilibrium equation yields an approximate solution in terms of the variables at time  $t$ . An incremental approach is often used to obtain the solution. The balance of momentum at time  $t + \Delta t$  is expressed as

$$\begin{aligned} & \int_{t+\Delta t V} {}^{t+\Delta t} \sigma_{ij} \frac{\partial \delta u_i}{\partial {}^{t+\Delta t} x_j} {}^{t+\Delta t} dV + \int_{t+\Delta t V} {}^{t+\Delta t} \rho {}^{t+\Delta t} \dot{v}_i \delta u_i {}^{t+\Delta t} dV \\ & = \int_{t+\Delta t V} {}^{t+\Delta t} f_i^B \delta u_i {}^{t+\Delta t} dV + \int_{t+\Delta t S} {}^{t+\Delta t} \sigma_{ij} \delta u_i {}^{t+\Delta t} n_j {}^{t+\Delta t} dS \end{aligned} \quad (9)$$

where  ${}^{t+\Delta t} \sigma_{ij}$  are the components of the cauchy stress tensor at time  $t + \Delta t$  and  ${}^{t+\Delta t} f_i^B$  are the components of the body force per unit mass at time  $t + \Delta t$ .

### Incremental decomposition

By referring all variables at time  $t + \Delta t$  to the grid configuration at time  $t$ , the variables can be expressed as their value at time  $t$  plus an increment of the variable during the time increment  $\Delta t$ . Material density at time  $t + \Delta t$  can be decomposed into

$${}^{t+\Delta t} \rho = {}^t \rho + {}^t \rho' \Delta t \quad (10)$$

Substituting (8) into (10) gives

$${}^{t+\Delta t} \rho = {}^t \rho - ({}^t \rho \frac{\partial {}^t v_k}{\partial {}^t x_k} + {}^t c_k \frac{\partial {}^t \rho}{\partial {}^t x_k}) \Delta t \quad (11)$$

Similarly, the stress components can be decomposed;

$${}^{t+\Delta t}\sigma_{ij} = {}^t\sigma_{ij} + {}^t\sigma'_{ij}\Delta t \quad (12)$$

Using (6), the grid time derivative of stress components can be expressed as

$${}^t\sigma'_{ij} = {}^t\dot{\sigma}_{ij} - {}^tc_k \frac{\partial {}^t\sigma_{ij}}{\partial {}^tx_k} \quad (13)$$

The material time derivative of cauchy stress  ${}^t\dot{\sigma}_{ij}$  is substituted from the material constitutive equation. The volume element at time  $t + \Delta t$  is related to the volume element at time  $t$  through

$${}^{t+\Delta t}dV = {}^tdV + {}^tdV'\Delta t \quad (14)$$

Similarly, elemental surface area at time  $t + \Delta t$  is related to elemental area at time  $t$  through

$${}^{t+\Delta t}(n_j dS) = {}^tn_j {}^tdS + ({}^tn_j {}^tdS)'\Delta t \quad (15)$$

We know from reference [8]:

$${}^tdV' = \frac{\partial {}^tv_k^g}{\partial {}^tx_k} {}^tdV \quad (16)$$

and

$$({}^tn_j {}^tdS)' = \frac{\partial {}^tv_k^g}{\partial {}^tx_k} {}^tn_j {}^tdS - \frac{\partial {}^tv_k^g}{\partial {}^tx_j} ({}^tn_k {}^tdS) \quad (17)$$

By substituting (16) and (17) into (14) and (15), respectively, we have

$${}^{t+\Delta t}dV = {}^tdV + \frac{\partial {}^tv_k^g}{\partial {}^tx_k} {}^tdV\Delta t \quad (18)$$

and

$${}^{t+\Delta t}(n_j dS) = {}^tn_j {}^tdS + \left( \frac{\partial {}^tv_k^g}{\partial {}^tx_k} {}^tn_j {}^tdS - \frac{\partial {}^tv_k^g}{\partial {}^tx_j} {}^tn_k {}^tdS \right) \Delta t \quad (19)$$

### Linearization

By substituting equations (10) to (19) into equation (9), the linearized form of this equation is obtained after higher order differential terms are neglected. The right hand side (RHS) of (9) may be written as

$$RHS = \int_{{}^{t+\Delta t}V} {}^{t+\Delta t}f_i^B \delta u_i {}^{t+\Delta t}dV + \int_{{}^{t+\Delta t}S} {}^{t+\Delta t}\sigma_{ij} \delta u_i {}^{t+\Delta t}n_j {}^{t+\Delta t}dS \quad (20)$$

After substituting of equations (11), (13), (18) and (19) into equation (20), RHS is expanded as

$$\begin{aligned} RHS = & \int_{{}^{t+\Delta t}V} \delta u_i [{}^tf_i^B + ({}^tf_i^B - {}^tc_k \frac{\partial {}^tf_i^B}{\partial {}^tx_k})\Delta t] \\ & (1 + \frac{\partial {}^tv_k^g}{\partial {}^tx_k} \Delta t) {}^tdV + \\ & \int_{{}^{t+\Delta t}S} \delta u_i [{}^t\sigma_{ij} + ({}^t\dot{\sigma}_{ij} - {}^tc_k \frac{\partial {}^t\sigma_{ij}}{\partial {}^tx_k})\Delta t] \\ & [{}^tn_j {}^tdS + (\frac{\partial {}^tv_k^g}{\partial {}^tx_k} {}^tn_j {}^tdS - \frac{\partial {}^tv_k^g}{\partial {}^tx_j} {}^tn_k {}^tdS)\Delta t] \end{aligned} \quad (21)$$

By simplifying the equation (21) and neglecting the higher order terms, we have

$$\begin{aligned} RHS = & \int_{{}^tV} \delta u_i {}^tf_i^B {}^tdV + \int_{{}^tS} \delta u_i {}^t\sigma_{ij} {}^tn_j {}^tdS + \\ & \{ \int_{{}^tV} \delta u_i ({}^t\dot{f}_i^B - {}^tc_k \frac{\partial {}^t\dot{f}_i^B}{\partial {}^tx_k} + {}^t\dot{f}_i^B \frac{\partial {}^tv_k^g}{\partial {}^tx_k}) {}^tdV + \\ & \int_{{}^tS} \delta u_i [({}^t\dot{\sigma}_{ij} - {}^tc_k \frac{\partial {}^t\sigma_{ij}}{\partial {}^tx_k}) {}^tn_j \\ & + {}^t\sigma_{ij} (\frac{\partial {}^tv_k^g}{\partial {}^tx_k} {}^tn_j - \frac{\partial {}^tv_k^g}{\partial {}^tx_j} {}^tn_k)] {}^tdS \} \Delta t \end{aligned} \quad (22)$$

From (9), the left hand side (LHS) becomes

$$\begin{aligned} LHS = & \int_{{}^{t+\Delta t}V} {}^{t+\Delta t}\sigma_{ij} \frac{\partial \delta u_i}{\partial {}^{t+\Delta t}x_j} {}^{t+\Delta t}dV + \\ & \int_{{}^{t+\Delta t}V} \rho {}^{t+\Delta t}\dot{v}_i \delta u_i {}^{t+\Delta t}dV = LHS1 + LHS2 \end{aligned} \quad (23)$$

For simplified treatment of the equation (23), it is divided in two parts, and each part is linearized separately. By substituting the incremental decomposition equations (11), (13) and (18) into LHS1, we have

$$\begin{aligned} LHS1 = & \int_{{}^tV} [{}^t\sigma_{ij} + ({}^t\dot{\sigma}_{ij} - {}^tc_k \frac{\partial {}^t\sigma_{ij}}{\partial {}^tx_k})\Delta t] \\ & [\frac{\partial \delta u_i}{\partial {}^tx_j} - (\frac{\partial \delta u_i}{\partial {}^tx_k} \frac{\partial {}^tv_k^g}{\partial {}^tx_j})\Delta t] (1 + \frac{\partial {}^tv_k^g}{\partial {}^tx_k} \Delta t) {}^tdV \end{aligned} \quad (24)$$

This is simplified to

$$\begin{aligned} LHS1 = & \{ \int_{{}^tV} \frac{\partial \delta u_i}{\partial {}^tx_j} [({}^t\dot{\sigma}_{ij} - {}^t\sigma_{ik} \frac{\partial {}^tv_k^g}{\partial {}^tx_k}) + \\ & {}^t\sigma_{ij} \frac{\partial {}^tv_k^g}{\partial {}^tx_k} - {}^tc_k \frac{\partial {}^t\sigma_{ij}}{\partial {}^tx_k}] {}^tdV \} \Delta t + \int_{{}^tV} {}^t\sigma_{ij} \frac{\partial \delta u_i}{\partial {}^tx_j} {}^tdV \end{aligned} \quad (25)$$

The second part of the LHS, which includes the inertial terms, can be similarly expanded using the incremental decomposition (11), (13) and (18)

$$LHS2 = \int_{\mathcal{V}} \delta u_i {}^{t+\Delta t} \dot{v}_i \left[ {}^t \rho - ({}^t \rho \frac{\partial {}^t v_k}{\partial {}^t x_k} + {}^t c_k \frac{\partial {}^t \rho}{\partial {}^t x_k}) \Delta t \right] \\ (1 + \frac{\partial {}^t v_k}{\partial {}^t x_k} \Delta t) {}^t dV \quad (26)$$

which is reduced to

$$LHS2 = \int_{\mathcal{V}} \delta u_i {}^{t+\Delta t} \dot{v}_i \left[ {}^t \rho - \frac{\partial ({}^t \rho {}^t c_k)}{\partial {}^t x_k} \Delta t \right] {}^t dV \quad (27)$$

The material acceleration  ${}^{t+\Delta t} \dot{v}$  in equation (27) may be expressed in terms of the referential acceleration  ${}^t \dot{v}'_i$  in the ALE reference configuration

$${}^{t+\Delta t} \dot{v}_i = {}^t \dot{v}_i + ({}^t \dot{v}'_i) \Delta t \quad (28)$$

By expanding the second term at right hand side of equation (28), we have

$${}^{t+\Delta t} \dot{v}_i = {}^t \dot{v}_i + ({}^t \dot{v}'_i) \Delta t - ({}^t c_j \frac{\partial {}^t v_i}{\partial x_j}) \Delta t \quad (29)$$

Equation (29) is substituted into equation (27), to yield

$$LHS2 = \int_{\mathcal{V}} \delta u_i ({}^t \dot{v}_i + ({}^t \dot{v}'_i) \Delta t - ({}^t c_j \frac{\partial {}^t v_i}{\partial x_j}) \Delta t) \\ ({}^t \rho - \frac{\partial ({}^t \rho {}^t c_k)}{\partial {}^t x_k} \Delta t) {}^t dV \quad (30)$$

Further simplification is achieved when multiplications are carried out and higher order terms are neglected

$$LHS2 = \int_{\mathcal{V}} \delta u_i {}^t \dot{v}_i {}^t \rho {}^t dV + \left\{ \int_{\mathcal{V}} \delta u_i (({}^t \dot{v}'_i) - ({}^t c_j \frac{\partial {}^t v_i}{\partial x_j})) {}^t \rho {}^t dV - \int_{\mathcal{V}} \delta u_i {}^t \dot{v}_i \frac{\partial ({}^t \rho {}^t c_k)}{\partial {}^t x_k} {}^t dV \right\} \Delta t \quad (31)$$

Also at time  $t$  the principal of virtual work is expressed as

$$\int_{\mathcal{V}} {}^t \sigma_{ij} \frac{\partial \delta u_i}{\partial {}^t x_j} {}^t dV + \int_{\mathcal{V}} {}^t \rho {}^t \dot{v}_i \delta u_i {}^t dV = \\ \int_{\mathcal{V}} {}^t f_i^B \delta u_i {}^t dV + \int_{\mathcal{S}} {}^t \sigma_{ij} \delta u_i {}^t n_j {}^t dS \quad (32)$$

Equation (22), (25) and (31) are combined to obtain the fully coupled ALE equation of motion. For this purpose,  $\Delta t$  is cancelled out from the equations and the principle of virtual work at time  $t$  is given by

$$\int_{\mathcal{V}} \frac{\partial \delta u_i}{\partial {}^t x_j} [({}^t \sigma_{ij} - {}^t \sigma_{ik} \frac{\partial {}^t v_j}{\partial {}^t x_k}) + {}^t \sigma_{ij} \frac{\partial {}^t v_k}{\partial {}^t x_k} - {}^t c_k \frac{\partial {}^t \sigma_{ij}}{\partial {}^t x_k}] {}^t dV + \\ \int_{\mathcal{V}} \delta u_i ({}^t \dot{v}_i) {}^t \rho {}^t dV = \\ \delta {}^{t+\Delta t} w^{ext} + \int_{\mathcal{V}} \delta u_i ({}^t c_j \frac{\partial {}^t v_i}{\partial {}^t x_j}) {}^t \rho {}^t dV + \\ + \int_{\mathcal{V}} \delta u_i {}^t \dot{v}_i \frac{\partial ({}^t \rho {}^t c_k)}{\partial {}^t x_k} {}^t dV \quad (33)$$

where

$$\delta {}^{t+\Delta t} w^{ext} = \int_{\mathcal{V}} \delta u_i ({}^t f_i^B - {}^t c_k \frac{\partial {}^t f_i^B}{\partial {}^t x_k} + {}^t f_i^B \frac{\partial {}^t v_k}{\partial {}^t x_k}) {}^t dV + \int_{\mathcal{S}} \delta u_i [({}^t \sigma_{ij} - {}^t c_k \frac{\partial {}^t \sigma_{ij}}{\partial {}^t x_k}) {}^t n_j + {}^t \sigma_{ij} (\frac{\partial {}^t v_k}{\partial {}^t x_k} {}^t n_j - \frac{\partial {}^t v_k}{\partial {}^t x_j} {}^t n_k)] {}^t dS \quad (34)$$

This form of treatment of ALE equation has been previously presented by Wang et al. [8] for quasi-static analysis and by Bayoumi and Gadala [1,13] for dynamic analysis. However, the present formulation has the following differences with the above reference:

a) In reference [13], linearization of equation of motion is carried out using the relationships:  ${}^{t+\Delta t} v_i^g = {}^t v_i^g + v_i^g$  and  ${}^{t+\Delta t} v_i = {}^t v_i + v_i$ . Later, the incremental material and grid velocities are linearized again to yield displacements. In other words, linearization is performed twice to relate the convective velocity at time  $t + \Delta t$  to displacement at time  $t$ . This operation has introduced an extra term to the final equation.

b) In the dynamic analysis, it is not generally necessary to linearize the velocity and acceleration at time  $t + \Delta t$  because the time incrementation of the velocity and acceleration at time  $t + \Delta t$  is achieved using methods such as Newmark's. Unlike reference [13], here, velocities and accelerations at time  $t + \Delta t$  are maintained in the equation during linearization. Then, after discretization of the equation, the Newmark method is used to obtain the time marching equation of motion. This general method reduces the computational time considerably, as the calculations to obtain the relationships between incremental displacements, velocities, and accelerations for the material and the grid in the Newmark approach are avoided.

c) A requirement which verifies the consistency of an ALE formulation is that it should be able to reduce to Lagrangian and Eulerian formulations as special cases

when proper mesh motion conditions are applied. The formulation in reference [8] satisfies this requirement for the quasi static case, but this reduction is not presented in for the dynamic formulation for the Eulerian case. The formulation presented in this work reduces to updated Lagrangian and Eulerian cases under proper conditions.

#### 4. MESH MOTION

In the ALE method, the finite element mesh can be moved arbitrarily to maintain a homogenous mesh and to properly represent boundary conditions throughout the deformation process. Following references [9, 10], a simple mesh motion scheme is used in this work that expresses the relationship between material and mesh displacement as

$$u_i^g = a_i + B_{ij}u_j \quad (35)$$

where the  $a_i$  and  $B_{ij}$  are vector and matrix of mesh motion parameters, respectively. This modified form of mesh motion equation allows a coupling between degrees of freedom of nodes, and is essential for specification of mesh sliding on external boundaries. Using this scheme, different types of motion are realized by following parameter selections,

Pure Lagrangian motion:  $a_i = 0$  and  $B_{ij} = \delta_{ij}$  i.e.,

$$v_i^g = v_i$$

Pure Eulerian motion:  $a_i = 0$  and  $B_{ij} = 0$  then  $v_i^g = 0$

General ALE motion:  $a_i$  and  $B_{ij}$  are arbitrary then  $v_i^g = arbitrary$  (specified by the mesh motion scheme)

The Transfinite mapping method [11] is one of the methods that may be utilized to specify mesh motion in Eq. (35). The transfinite mesh generation method is originally designed for creating a mesh on a geometric region with specified boundaries.

If the mapping of a typical distorted mesh region for the borders of a quadrilateral region are defined as  $\phi_i(r,0)$ ,  $\phi_i(r,1)$ ,  $\phi_i(0,s)$  and  $\phi_i(1,s)$ , then the coordinates of an interior new mesh point can be obtained by mapping the region onto a unit square: (see Figure 2)

$$\begin{aligned} {}^{t+\Delta t}x_i(r,s) = & (1-s)\phi_i(r,0) + s\phi_i(r,1) + \\ & (1-r)\phi_i(0,s) + r\phi_i(1,s) - (1-r)(1-s)\phi_i(0,0) \\ & - (1-r)s\phi_i(0,1) - rs\phi_i(1,1) - r(1-s)\phi_i(1,0) \end{aligned} \quad (36)$$

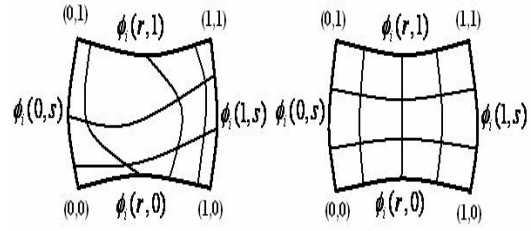


Figure 2: Transfinite mapping of a distorted mesh region bounded by four curves

where  $(r,s)$  are normalized coordinates ( $0 \leq r \leq 1$  and  $0 \leq s \leq 1$ ). Therefore, the parameter  $a_i$  for an internal degree of freedom of the mesh is obtained from

$$a_i = {}^{t+\Delta t}x_i - {}^t x_i \quad (37)$$

#### 5. FINITE ELEMENT EQUATIONS

The ALE finite element equations are obtained from discretization of equation (33). The final form of this equation may be cast in the standard form as

$${}^t K v + {}^t K^g v^g = f \quad (38)$$

where  ${}^t K$  is the stiffness matrix related to material deformation,  ${}^t K^g$  is the stiffness matrix resulting from grid motion, and  $f$  is the load vector. We note that  ${}^t K$  includes inertia terms which result from the application of Newmark implicit integration scheme. Also, we have used the Juamman stress rate tensor for the material rate of Cauchy stresses.

The grid displacements can be condensed out of the equation of motion at the element level by substituting the mesh motion equation

$$u^g = a + B u \quad (39)$$

into equation (38), which results in

$$({}^t K - {}^t K^g) u = f + {}^t K^g a \quad (40)$$

After assembling the element equations into global equations, the conventional finite element solution techniques may be applied to solve for material displacements.

#### 6. STRESS UPDATE SCHEME

In this work, we use a hypoelastoplastic model that is based on an additive decomposition of the rate of deformation tensor  $D_{ij}$  into elastic and plastic parts

$${}^t D_{ij} = {}^t D_{ij}^E + {}^t D_{ij}^P \quad (41)$$

where

$${}^t D_{ij} = \frac{1}{2} \left( \frac{\partial^t v_i}{\partial^t x_j} + \frac{\partial^t v_j}{\partial^t x_i} \right) \quad (42)$$

In the hypoelastoplastic model, an objective stress rate should be used to provide the objectivity of constitutive equation. This equation may be written as

$$\overset{\nabla}{\sigma}_{ij} = C^e_{ijkl} D^e_{kl} = C^e_{ijkl} (D_{kl} - D^p_{kl}) \quad (43)$$

where  $\overset{\nabla}{\sigma}_{ij}$  is an objective rate of stress, e.g. Jaumann rate of Cauchy stress, and  $C^e_{ijkl}$  is the linear isotropic elastic tensor. Assuming Mises plasticity with isotropic hardening, the plastic potential is expressed as a function of stress and equivalent plastic strain

$$f = \bar{\sigma} - \sigma_Y(\bar{\varepsilon}^p) \quad (44)$$

$\bar{\sigma}$  is the equivalent stress and  $\dot{\bar{\varepsilon}}^p$  is the equivalent plastic strain rate.

In a large deformation analysis, the integration of the constitutive equations should be carried out in a way that the objectivity of the constitutive equations is preserved. In this work, we use the common return mapping algorithm to satisfy the plastic consistency condition. This method consists of an elastic predictor phase, in which a trial stress is computed at time  $t + \Delta t$  by assuming pure elastic deformation, followed by a plastic corrector phase in which the trial stress is projected onto an updated yield surface in order to satisfy the plastic consistency condition. In the ALE method, however, integration and material points are not coincident, so the stress needs to be updated using the relative velocity as given by Eq. (12).

Furthermore, since, the material and grid points are not necessarily coincident in the ALE method, it is necessary to update the material properties at each time step from material integration points to grid points. Updating of a physical quantity  $f$  from a material point to a mesh point can be performed using the following equation

$${}^{t+\Delta t} f^g = {}^{t+\Delta t} f + \frac{\partial {}^{t+\Delta t} f}{\partial {}^{t+\Delta t} x_i} (u_i^g - u_i) \quad (45)$$

## 7. APPLICATION: STATIC AND DYNAMIC PUNCH INDENTATION

To illustrate the effectiveness of the ALE method in dynamic analysis, an example of punch indentation process solved by this approach is presented here. This example shows the robustness of this formulation in handling contact boundary conditions and in preventing mesh distortion. Both static and dynamic analyses are presented to show the significance of dynamic effects. Figure 3 shows the geometry and initial mesh of the

material. The material is assumed to be an elastic-plastic linear-hardening material with a Young's modulus of 200 GPa, a Poisson's ratio of 0.3, an initial yield stress of 250 MPa and a hardening parameter of 1.0 GPa.

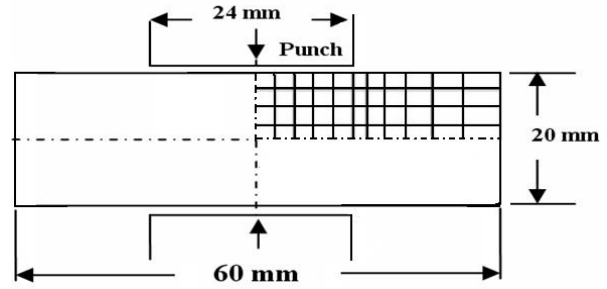


Figure 3: Geometry and initial mesh for punch indentation

Figure 4 shows the evolution of the deformed shape obtained using the developed ALE formulation in static case. The figure shows that the contact condition between the punch and the workpiece is accurately satisfied. This was easily achieved by setting the degrees of freedom of the nodes directly under the punch to be Lagrangian in the vertical direction (to satisfy the boundary constraint) and Eulerian in the horizontal direction (to maintain the nodes under the punch). In this way, no special contact algorithm was needed to handle the contact conditions. In addition, using the designed mesh motion scheme, the ALE maintained a homogeneous mesh throughout the deformation history.

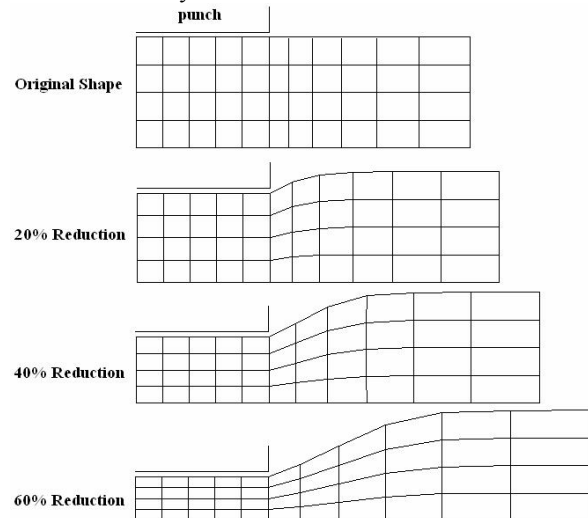


Figure 4: Evolution of the deformed shape during the punch indentation

Figure 5 shows the evolution of the yield stress during the deformation process for the dynamic cases at a punch velocity of  $v=60$  m/s. It is observed that the ALE formulation with proper mesh motion maintains mesh

regularity and allows for an accurate description of the boundary motion. The evolution of the plastic areas starts from the right corner of the tool.

To investigate the dynamic effects, several punch velocities are simulated. Figure 6 shows the comparison between the final deformed shapes for various velocities. The dynamic effects are negligible for velocities under 2 m/s, but as the punch moves down at a faster rate, the plastic deformation is further localized because there is a shorter time for the plastic wave to propagate in the bulk of material. In other words, the final shape of the workpiece is clearly dependent on the punch velocity.

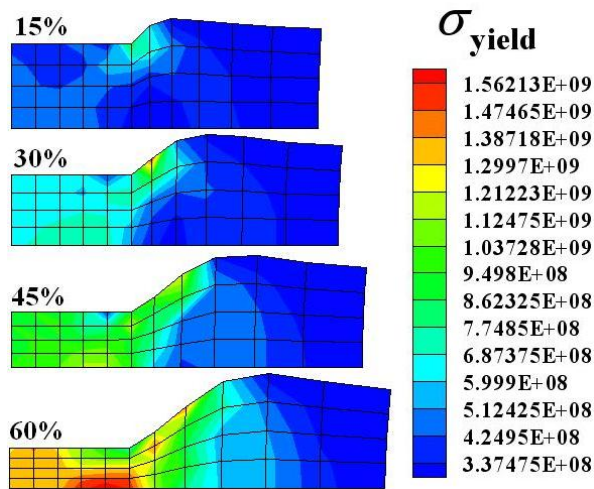


Figure 5: Evolution of the yield stress field during the deformation process

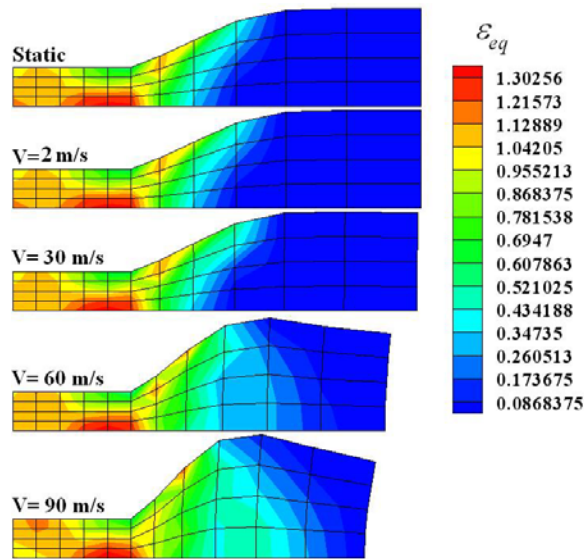


Figure 6: Deformed shape and equivalent plastic strain at different punch velocities

This type of problems is difficult to handle with a pure Lagrangian computation because several remeshing steps

are needed to overcome severe element distortions which are common to Lagrangian analysis. In addition, a contact algorithm may be needed to represent the motion of the die. Using the ALE method and its mesh motion scheme, the punch motion is simulated by directly applying appropriate velocity boundary conditions, and mesh distortion is avoided, resulting in a considerable computational saving.

The punch indentation problem has been repeatedly solved in the ALE literature, thus it is appropriate to compare the results with other references. It is apparent from Fig. 6. that the final length of the specimen ( $L$ ) and its maximum height ( $H$ ) are the two dimensions that are significantly affected by the punch speed. Therefore, they may be used as indicators for the forming of the specimen under dynamic loading.

TABLE 1

COMPARISON OF RESULTS FOR PUNCH INDENTATION		
Reference	Final _H(mm)	Final _L(mm)
Huerta A. and Gasadei F. [12]	11.0	36.5
Bayoumi H.N. and Gadala M.S. [13]	11.0	43.0
Current work	11.5	37.75

Table (1) compares the values of these parameters for the case of punch speed of 60 m/s and after a punch advancement equivalent to 60% of initial height. It is observed that while the maximum length are almost the same for all cases, the specimen height is between the two other values reported, being closer to the value given in reference [13]. Furthermore, the distribution of yield stress and plastic strains presented in figures 5 and 6 are similar to those reported in the references.

## 8. CONCLUSIONS

In this paper, an implicit fully coupled ALE formulation for nonlinear solid mechanics applications was presented. Starting from the basic principles of continuum mechanics, ALE equilibrium equations were derived for both quasi-static and dynamic analyses. The ALE equilibrium equation was linearized and used for simulation of large deformation processes in an incremental fashion. Examples of quasi-static and dynamic large deformation problems were simulated using this approach. The results show the effectiveness of the ALE approach in handling contact boundary conditions and in preventing mesh distortion. The influence of inertia effects on material deformation was also presented.

## 9. REFERENCES

- [1] M.S. Gadala, "Recent trends in ALE formulation and its applications in solid mechanics," *Appl. Mech. Engrg.* vol. 193, pp. 4247-4275, 2004.
- [2] Benson DJ., "An efficient, accurate, simple ALE method for nonlinear finite element programs," *Comput. Meth. Appl.Mech. Eng.* Vol. 72, pp. 305-350, 1989.
- [3] Haber RB., "A mixed Eulerian-Lagrangian displacement model for large-deformation analysis in solid mechanics," *Comput. Meth. Appl. Mech. Eng.* Vol. 43, pp. 277-292, 1984.
- [4] Hue'tink J, Vreede PT, van der Lugt J, "Progress in mixed Eulerian-Lagrangian finite element simulation of forming processes", *Int. J. Numer. Meth. Eng.* Vol. 30, pp. 1441-1457, 1990.
- [5] Kennedy JM, Belytschko TB, "Theory and application of a finite element method for arbitrary Lagrangian-Eulerian fluids and structures," *Nuc. Eng. Des.* Vol. 68, pp. 129-146, 1981.
- [6] Schreurs PJG, Veldpaus FE, Brekelmans WAM, "Simulation of forming processes using the arbitrary Eulerian- Lagrangian formulation," *Comput. Meth. Appl. Mech. Eng.* Vol. 58, pp. 19-36, 1986.
- [7] T.J.R. Hughes, W.K. Liu, T.K. Zimmermann, "Lagrangian-Eulerian finite element formulation for incompressible viscous flows," *Comput. Methods Appl. Mech. Engrg.* Vol. 29, pp. 329-349, 1981.
- [8] J. Wang, M.S. Gadala, "formulation and survey of ALE method in nonlinear solid mechanics," *Finite Element Anal. Des.* Vol. 24, pp. 253-269, 1997.
- [9] Gadala, M.S. and Wang, J., "Apractical procedure for mesh motion in ALE method," *Eng. With Computers*, Vol. 14, pp. 223-234, 1998.
- [10] M.S. Gadala, M.R. Movahhedy, J. Wang, "On the mesh motion for ALE modeling of metal forming processes," *Finite Elements in Analysis and Design*, Vol. 38, pp. 435-459, 2002.
- [11] R. Haber, M.S. Shepard, J.F. Abel, R.H. Gallagher, D.P. Greenberg, "A general two-dimensional, graphical finite element preprocessor utilizing discrete transfinite mapping," *Int. J. Numer. Methods Engrg.* Vol. 17, pp. 1015-1044, 1981.
- [12] A. Huerta, F. Casadei, "New ALE applications in non-linear fast-transient solid dynamics," *Engineering Computations*, Vol. 11, pp. 317-345, 1994.
- [13] H.N. Bayoumi, M.S. Gadala, "A complete finite element treatment for the fully coupled implicit ALE formulation," *Computational Mechanics*, Vol. 33, pp. 435-452, 2004..